

# MEASURING HIGGS BOSON SELF- COUPLINGS WITH $2 \rightarrow 3$ VBS

Junmou Chen (Jinan University, Guangdong)

at MIP2024

Based on 2105.11500, 2112.12507

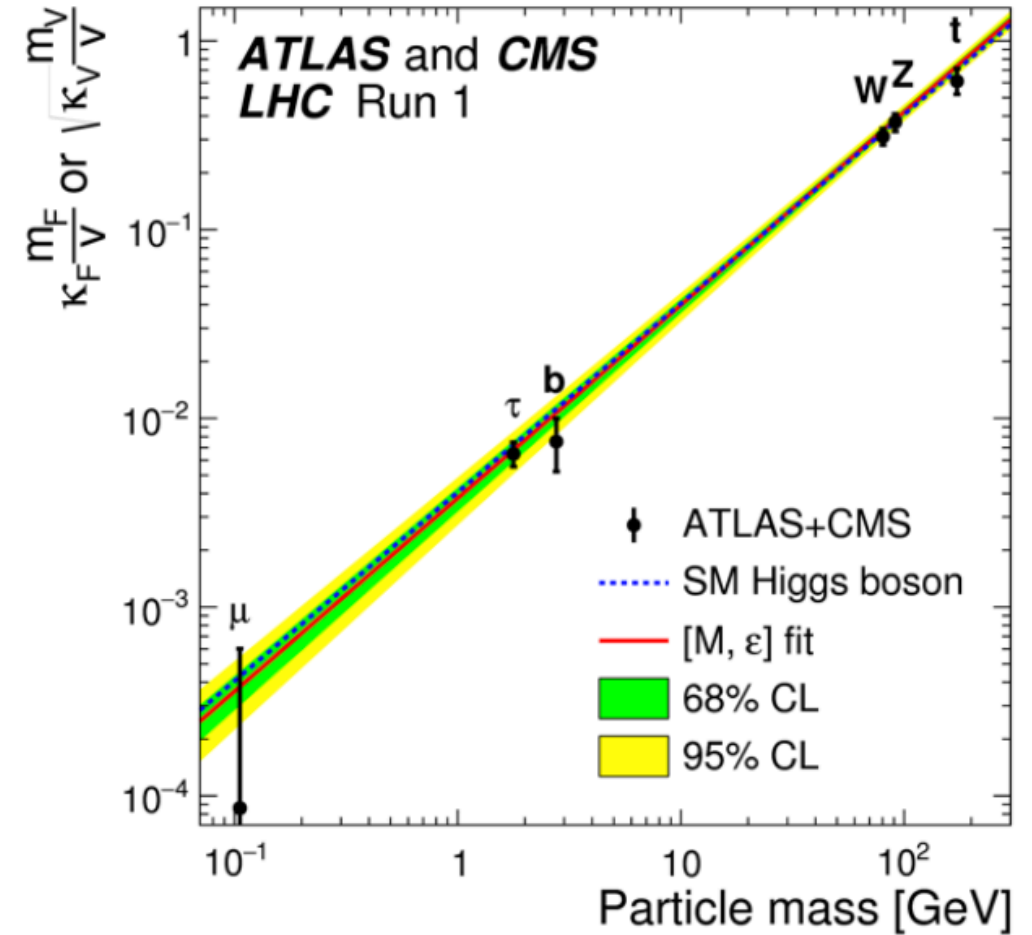
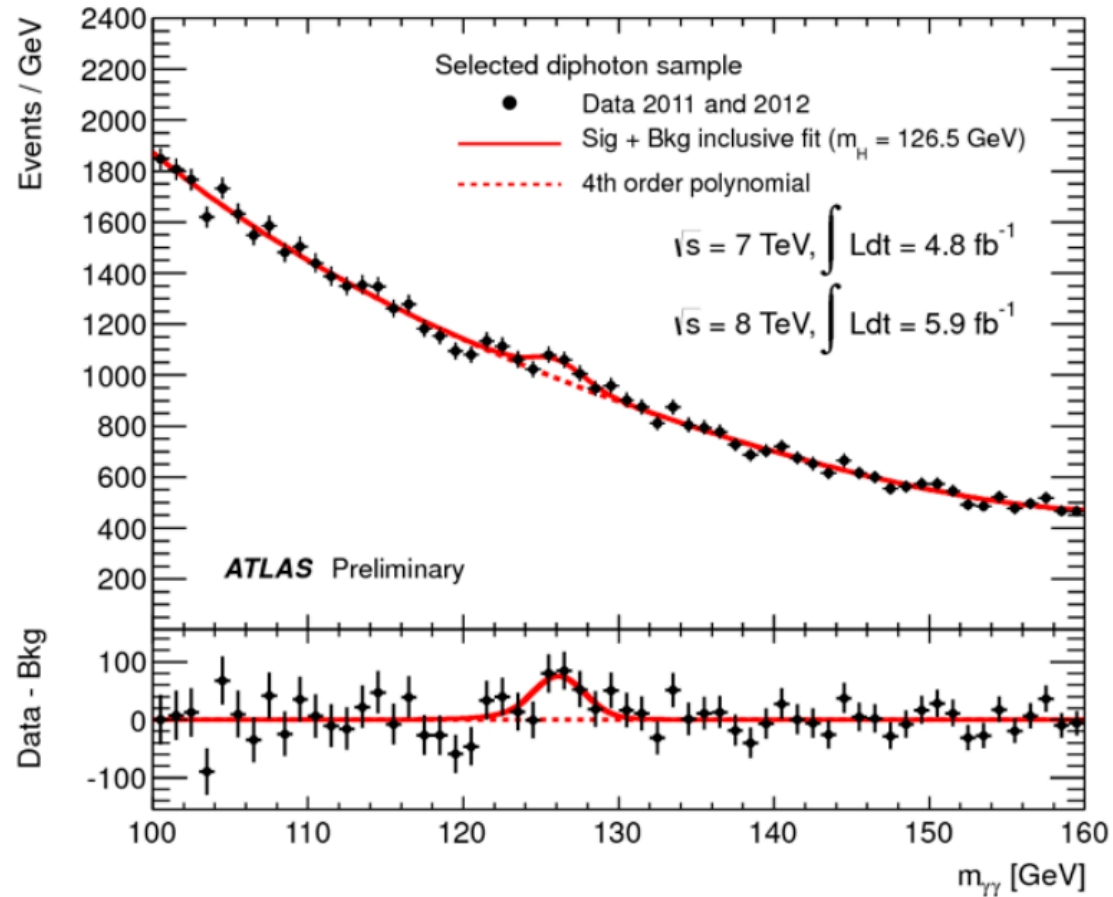
In collaboration with Yongcheng Wu, Chih-Ting Huang,  
Tong Li, Chang-Yuan Yao

# OUTLINE

- 1. Motivation
- 2. Physical Analysis and Strategy
- 3. Simulation and results

# Higgs Discovery – Completion of SM

## 1. Motivation

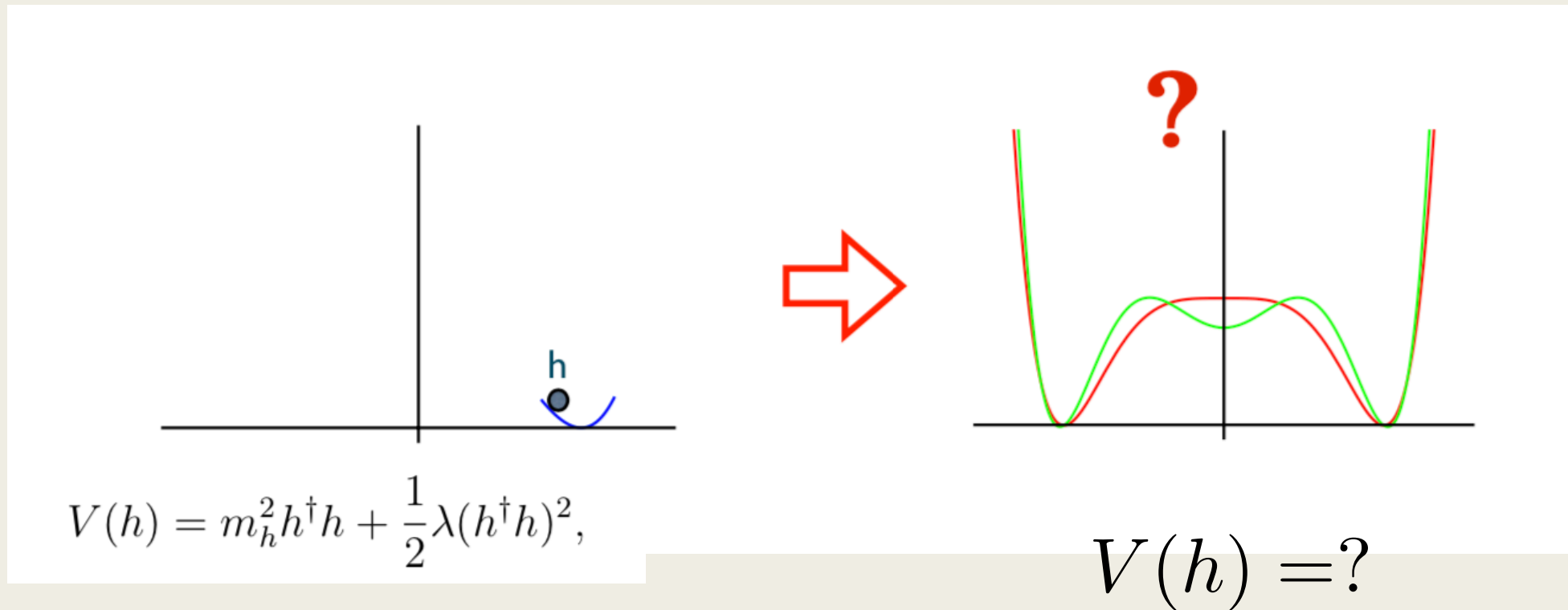


$$pp \rightarrow h \rightarrow \gamma\gamma$$

# UNFINISHED BUSINESS:

## 1. Motivation

- Many Higgs couplings haven't been not measured precisely
- Higgs self-couplings still haven't been not measured at all.
- Direct related the shape of Higgs Potential, and therefore the origin of EW symmetry breaking



# New Colliders

- Hadron collider: HE-LHC(27 TeV), 100 TeV and etc.

[1902.04070](#), 1902.00134, 1607.01831

- e+e- collider:

250 GeV-260 GeV: ILC, CEPC

1810.09037, 1903.01629

1-5 TeV: CLIC

*hep-ph/0412251*

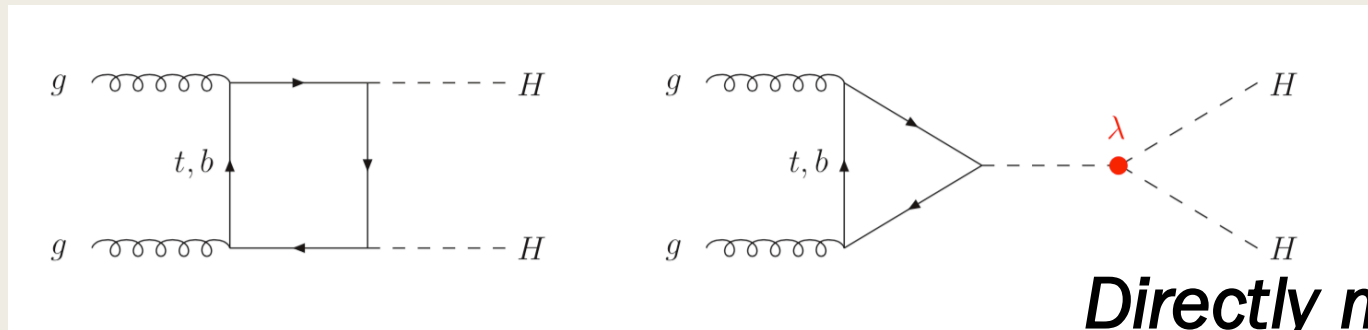
- Muon collider

3、 10、 14 TeV 2103.14043, 2303.08533

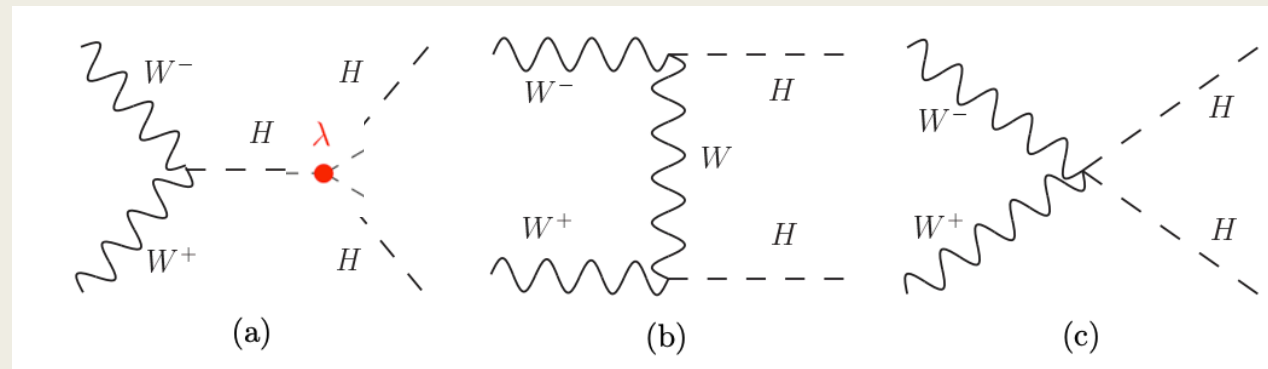
High energy & clean environment

# Main Channel for Higgs self-coupling measurement

- LHC:  $gg \rightarrow hh$  ( $pp \rightarrow hh$ )



- Future muon collider:  $WW/ZZ \rightarrow hh$  ( $\mu\mu \rightarrow \nu\nu(/\mu\mu)hh$ )



2008.12204

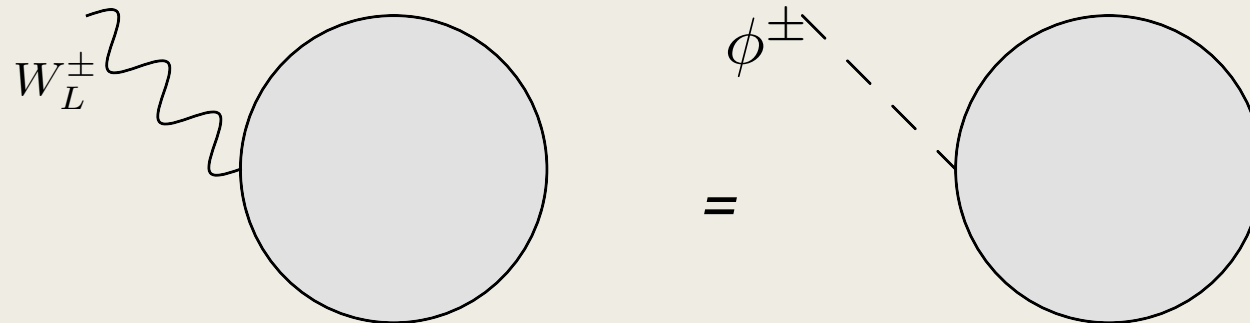
# Another approach:

## 1. Motivation

1. Higgs field in SM: Higgs boson and would-be Goldstone bosons form a SU(2) doublet:

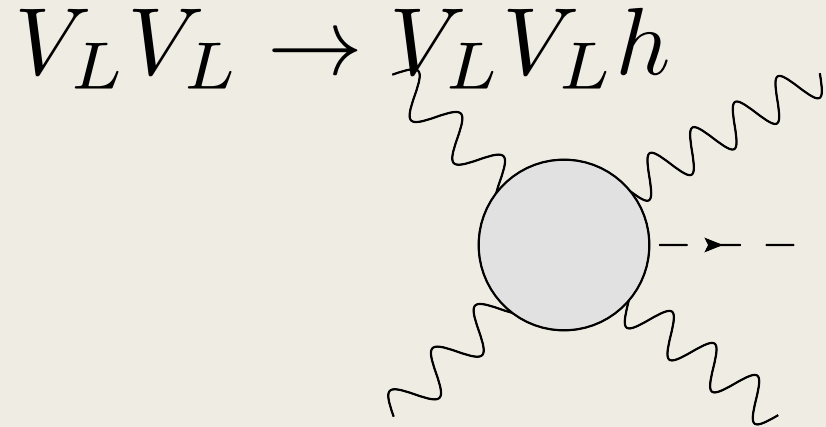
$$\Phi^\pm = \begin{pmatrix} \phi^\pm \\ \frac{1}{\sqrt{2}}(h + i\phi^0) \end{pmatrix}$$

2. Goldstone equivalence theorem



3. New approach: Measuring Higgs couplings through  $V_L$ .

# Our focus: $2 > 3$ Vector Boson Scattering

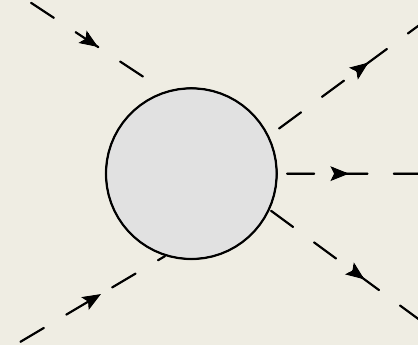


Proposed by Henning et.al.

in arxiv: 1812.09299 (Phys. Rev. Lett. **123**, 181801)

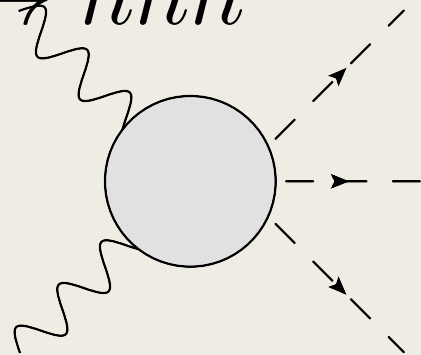
When  $E \gg m$

$\approx$



$V_L V_L \rightarrow h h h$

2003.13628



Take Goldstone equivalence (GET)

Muon collider especially suitable for this process



- Parameterization scheme: SMEFT.

## 2. SMEFT and Amplitudes

$$\mathcal{L} = \mathcal{L}_{\text{SM}} + \sum_i \frac{c_i \mathcal{O}_i}{\Lambda^2} + \mathcal{O}\left(\frac{1}{\Lambda^3}\right)$$

- Dim-6 operators related to Higgs physics

$$\begin{aligned} \mathcal{L}_{\text{dim-6}} = & \frac{1}{\Lambda^2} \left( c_6 (\Phi^\dagger \Phi)^3 + c_{\Phi_1} \partial^\mu (\Phi^\dagger \Phi) \partial_\mu (\Phi^\dagger \Phi) + c_{\Phi_2} (\Phi^\dagger D^\mu \Phi)^* (\Phi^\dagger D_\mu \Phi) \right. \\ & + c_{\Phi^2 W^2} \Phi^\dagger \Phi W_{\mu\nu}^a W^{a\mu\nu} + c_{\Phi^2 B^2} \Phi^\dagger \Phi B_{\mu\nu} B^{\mu\nu} + c_{\Phi^2 WB} \Phi^\dagger \tau^a \Phi W_{\mu\nu}^a B^{\mu\nu} \\ & \left. + c_{W^3} \epsilon^{abc} W_\mu^{a\nu} W_\nu^{b\rho} W_\rho^{b\mu} \right) \end{aligned}$$

- Under GET, only  $\mathcal{O}_6, \mathcal{O}_{\Phi_1}$  contribute to the Higgs self-coupling(s). Our focus.

### *2>3 VBS amplitude in high energy*

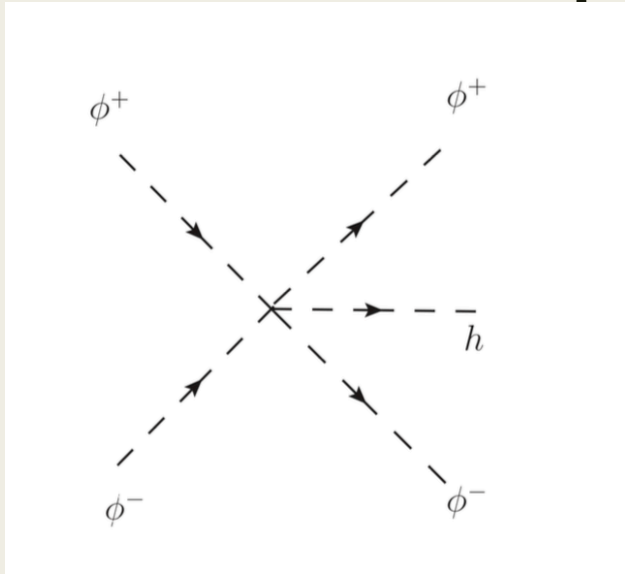
- In high energy limit, new physics is very sensitive to new physics for  $V_L V_L \rightarrow V_L V_L h$  &  $V_L V_L \rightarrow h h h$

- The amplitudes behave as

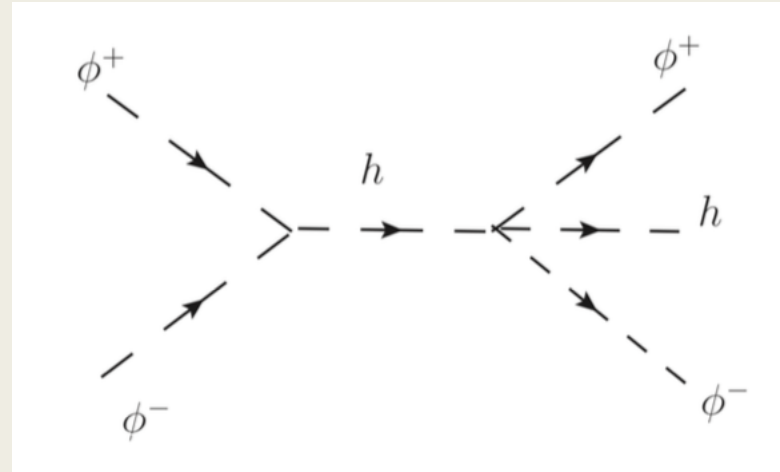
$$\frac{\mathcal{A}^{BSM}}{\mathcal{A}^{SM}} \sim \frac{E^2}{\Lambda^2}$$

## 2. SMEFT and Amplitudes

### Feynman diagrams(GET)

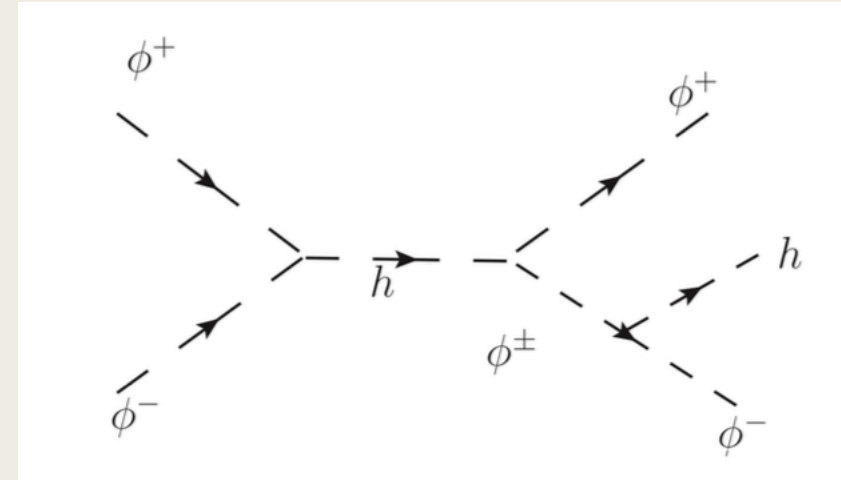


$$\mathcal{A}_0 \sim \frac{v}{\Lambda^2}.$$



$$\mathcal{A}_1^{SM} \sim \frac{v}{E^2}.$$

$$\mathcal{A}_1^{BSM} \sim \frac{v}{\Lambda^2}.$$

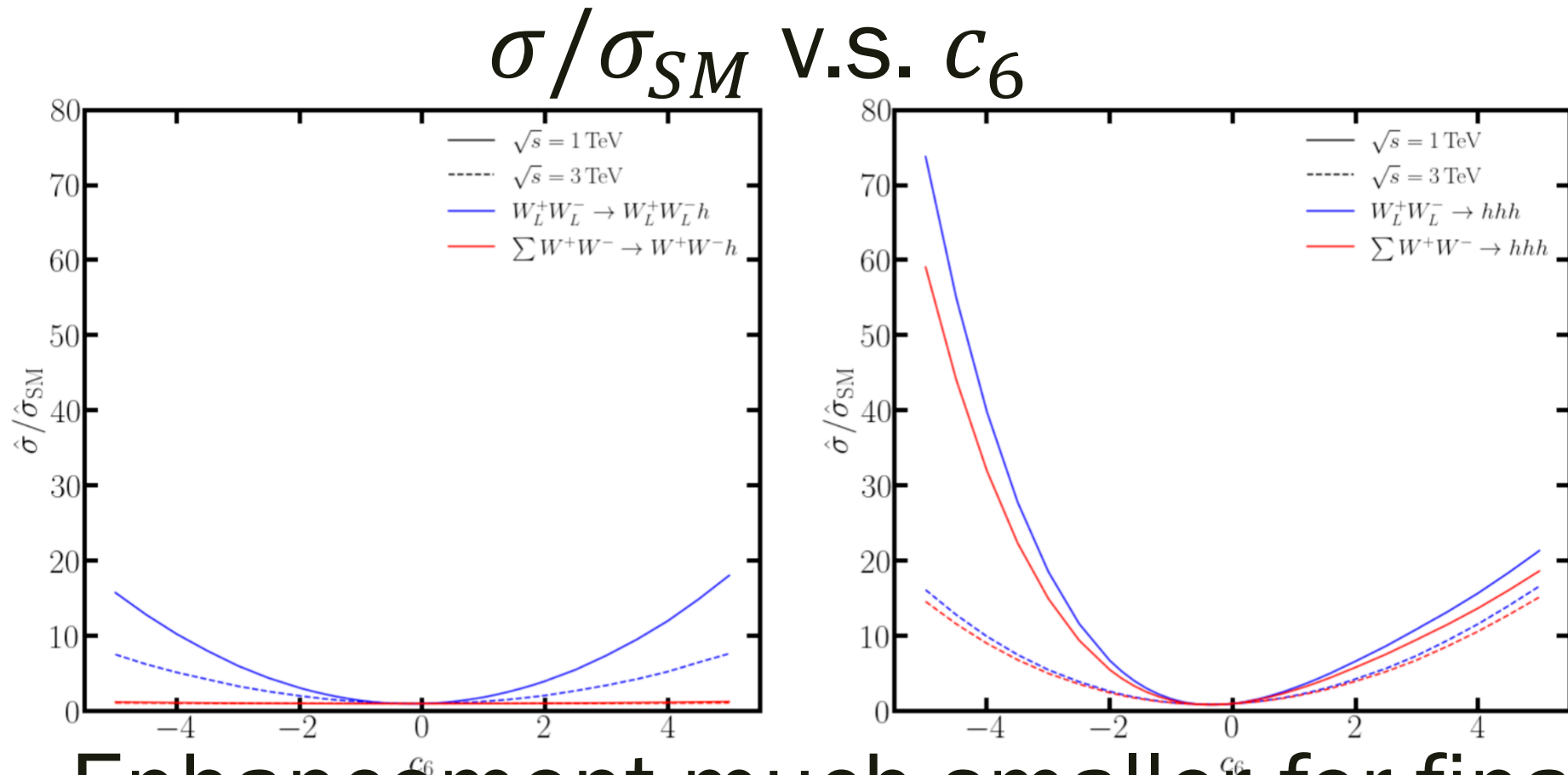


$$A_2 \simeq A_2^a + A_2^b + A_2^c \sim \frac{v}{\Lambda^2} + \frac{v}{E^2}$$

$$\mathcal{A}^{SM} \simeq \frac{v}{E^2} \quad \mathcal{A}^{BSM} \simeq \frac{v}{\Lambda^2}$$

$$\frac{\mathcal{A}^{BSM}}{\mathcal{A}^{SM}} \sim \frac{E^2}{\Lambda^2}$$

## 3.2 Partonic cross section 3. Cross Section and Constraints



Enhancement much smaller for final  $hh$ .

Figure 3.  $\hat{\sigma}/\hat{\sigma}_{SM}$  for  $W^+W^- \rightarrow W^+W^-h$  and  $W^+W^- \rightarrow hhh$  as functions of  $c_6$ .

## 3.2 Full Processes

## 3. Cross Section and Constraints

$$\begin{array}{ll} l^+l^- \rightarrow \nu_l\bar{\nu}_l W_L^+ W_L^- h & l^+l^- \rightarrow \nu_l\bar{\nu}_l h h h \\ pp \rightarrow jj W_L^\pm W_L^\pm h & pp \rightarrow jj h h h \end{array}$$

Lepton colliders: 1-30 TeV

Hadron colliders: 14, 27, 100 TeV

### Simulation settings:

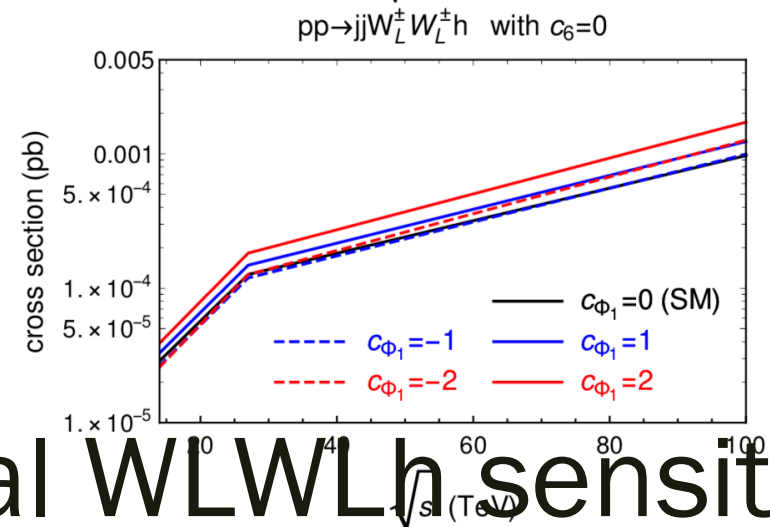
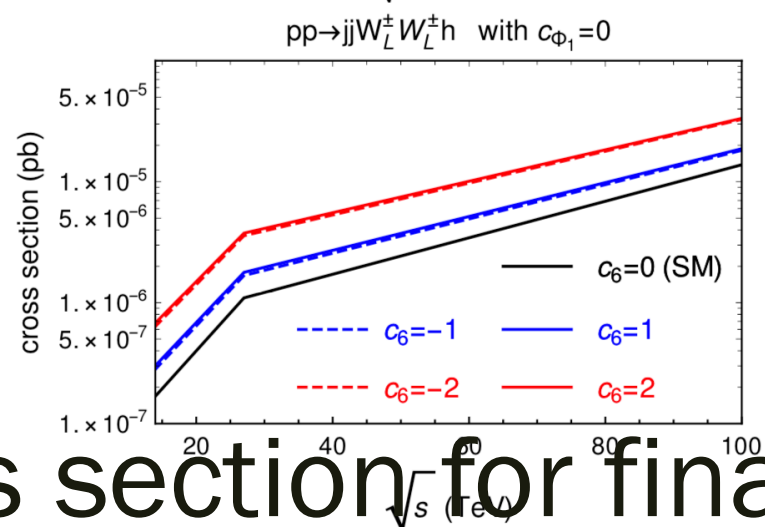
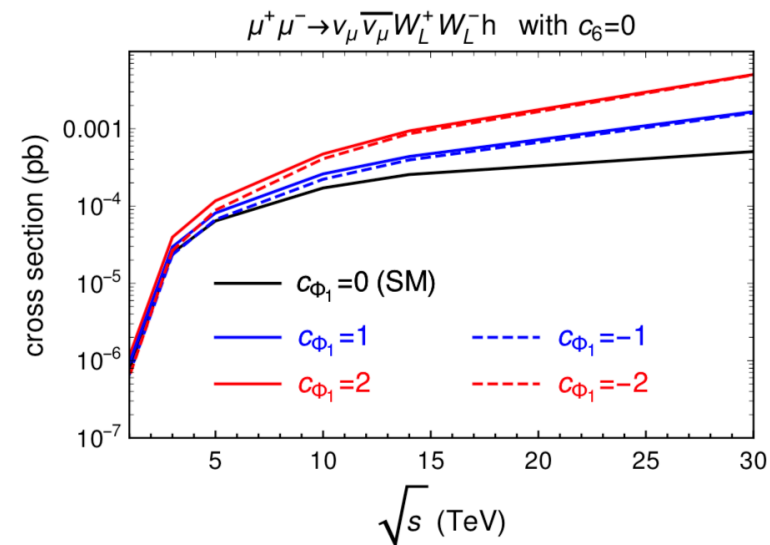
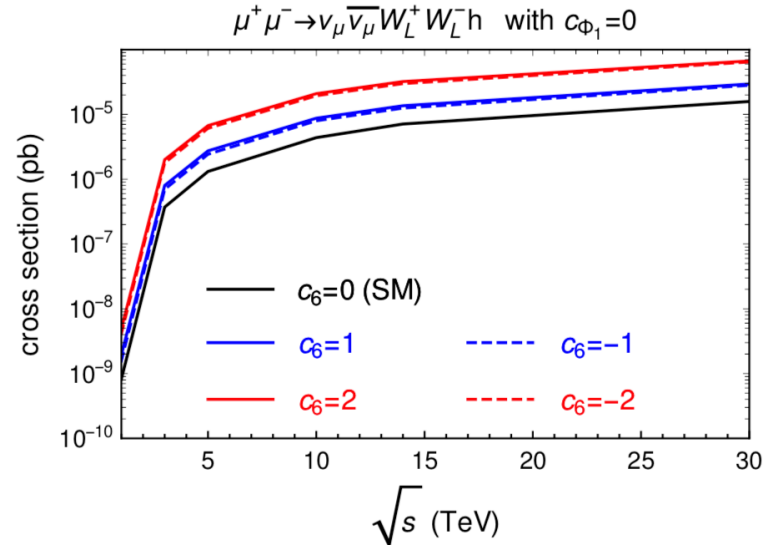
1. Select final vector bosons to be longitudinal
2. Impose PT cuts on final VL to reduce SM background.

Cross sections (pb) for $\mu^+\mu^- \rightarrow \nu_\mu\bar{\nu}_\mu W_L^+ W_L^- h$ with $c_{\Phi_1} = 0$					
$c_6$	-2	-1	0	1	2
1 TeV	$4.17 \times 10^{-9}$	$1.57 \times 10^{-9}$	$8.22 \times 10^{-10}$	$1.93 \times 10^{-9}$	$4.90 \times 10^{-9}$
3 TeV	$1.79 \times 10^{-6}$	$6.98 \times 10^{-7}$	$3.71 \times 10^{-7}$	$8.01 \times 10^{-7}$	$2.00 \times 10^{-6}$
5 TeV	$6.10 \times 10^{-6}$	$2.43 \times 10^{-6}$	$1.32 \times 10^{-6}$	$2.74 \times 10^{-6}$	$6.72 \times 10^{-6}$
10 TeV	$1.94 \times 10^{-5}$	$7.98 \times 10^{-6}$	$4.38 \times 10^{-6}$	$8.74 \times 10^{-6}$	$2.09 \times 10^{-5}$
14 TeV	$2.99 \times 10^{-5}$	$1.25 \times 10^{-5}$	$7.11 \times 10^{-6}$	$1.36 \times 10^{-5}$	$3.22 \times 10^{-5}$
30 TeV	$6.45 \times 10^{-5}$	$2.82 \times 10^{-5}$	$1.58 \times 10^{-5}$	$2.95 \times 10^{-5}$	$6.68 \times 10^{-5}$

**Table 1:** The cross section for  $\mu^+\mu^- \rightarrow \nu_\mu\bar{\nu}_\mu W_L^+ W_L^- h$  with  $c_{\Phi_1} = 0$  at different c.m. energies. Five benchmark points of  $c_6$  are displayed in different columns. The cuts  $m_{\nu\nu} > 150$  GeV,  $p_T(W, h) > 150$  GeV are implemented to obtain these cross sections.

Cross sections (pb) for $\mu^+\mu^- \rightarrow \nu_\mu\bar{\nu}_\mu W^+ W^- h$ with $c_{\Phi_1} = 0$					
$c_6$	-2	-1	0	1	2
1 TeV	$2.87 \times 10^{-8}$	$2.51 \times 10^{-8}$	$2.37 \times 10^{-8}$	$2.44 \times 10^{-8}$	$2.73 \times 10^{-8}$
3 TeV	$2.04 \times 10^{-5}$	$1.90 \times 10^{-5}$	$1.85 \times 10^{-5}$	$1.88 \times 10^{-5}$	$2.01 \times 10^{-5}$
5 TeV	$8.18 \times 10^{-5}$	$7.74 \times 10^{-5}$	$7.60 \times 10^{-5}$	$7.72 \times 10^{-5}$	$8.07 \times 10^{-5}$
10 TeV	$3.16 \times 10^{-4}$	$3.02 \times 10^{-4}$	$3.00 \times 10^{-4}$	$3.02 \times 10^{-4}$	$3.13 \times 10^{-4}$
14 TeV	$5.29 \times 10^{-4}$	$5.12 \times 10^{-4}$	$5.03 \times 10^{-4}$	$5.06 \times 10^{-4}$	$5.29 \times 10^{-4}$
30 TeV	$1.38 \times 10^{-3}$	$1.31 \times 10^{-3}$	$1.31 \times 10^{-3}$	$1.33 \times 10^{-3}$	$1.36 \times 10^{-3}$

# 3.2 Full Processes: simulation results



Cross section for final  $W_L W_L h$  sensitive to  $c_6$  and  $c_{\Phi_1}$ .

# Background Analysis

$$\mu^+\mu^- \rightarrow \nu_\mu\bar{\nu}_\mu W^+W^-h \quad (WW \text{ fusion}) .$$

Channel:  $W^\pm \rightarrow l^\pm \nu l$ ;  $W^\mp \rightarrow jj'$   $h \rightarrow b\bar{b}$

Signal:  $l^\pm jj' b\bar{b} + \text{MET}$

Background

$$\mu^+\mu^- \rightarrow t\bar{t}, \quad \nu_\mu\bar{\nu}_\mu t\bar{t}, \quad W^+W^-Z, \quad \nu_\mu\bar{\nu}_\mu W^+W^-Z \quad \text{and} \quad \gamma\gamma \rightarrow t\bar{t}$$



# 3.2 Constraints on $c_6$ and $c_{\Phi_1}$

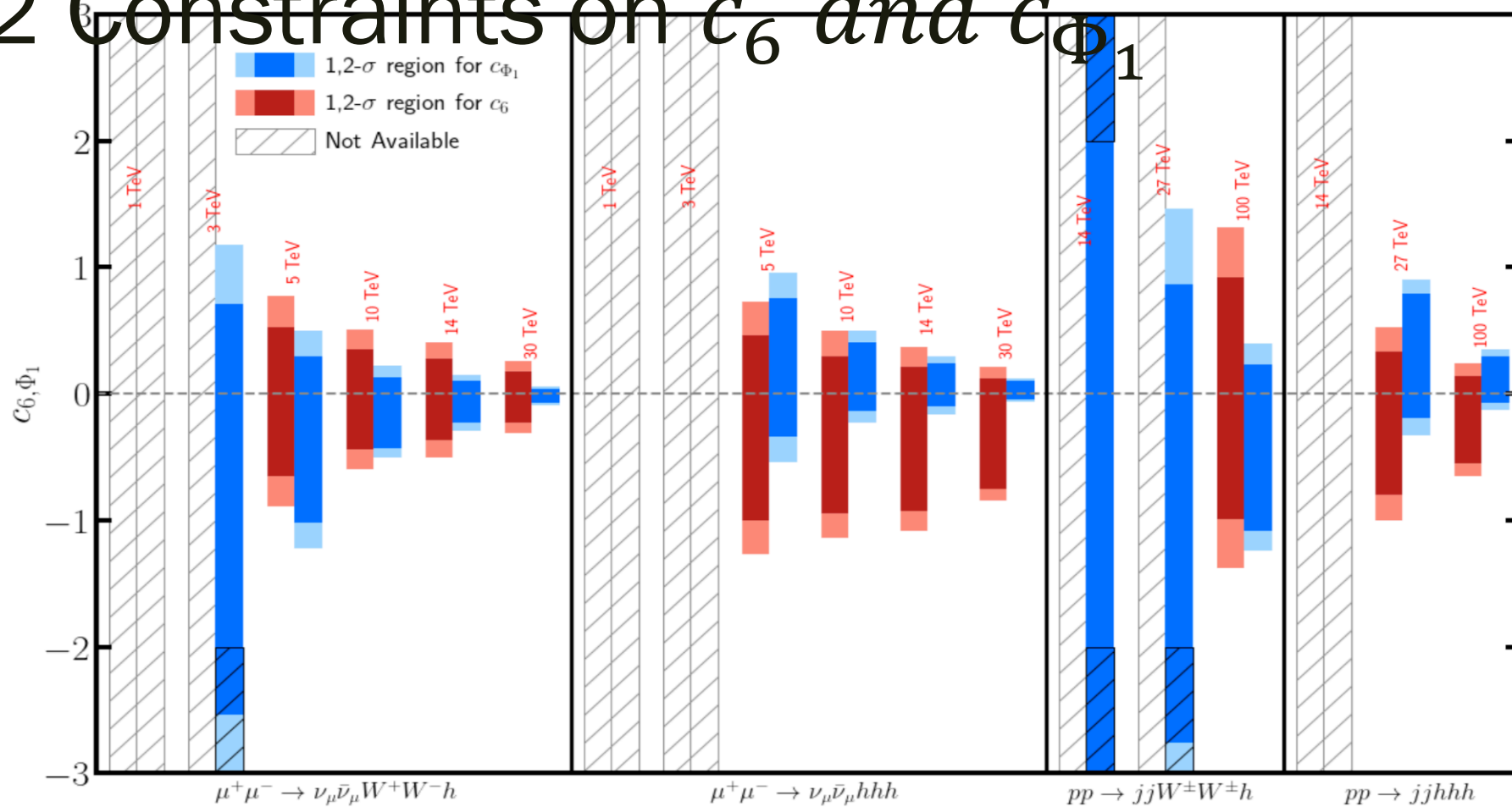


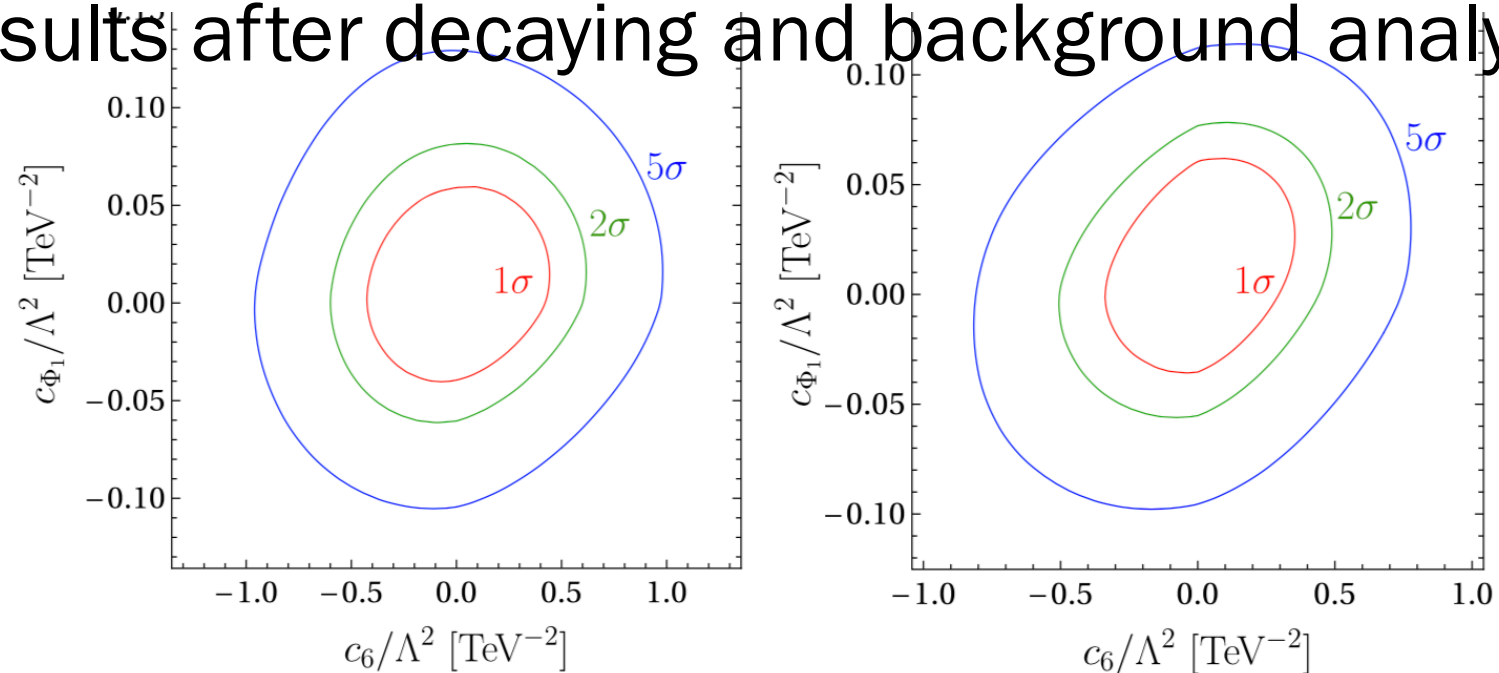
**Figure 12:** The allowed region for  $c_6$  (red) and  $c_{\Phi_1}$  (blue) from different channels. The darker color indicates the 1- $\sigma$  region, while lighter one indicates the 2- $\sigma$  region. The hatched region are not available either due to low event rate or beyond  $[-2, 2]$ .

Naive estimation: no decay, no background analysis.

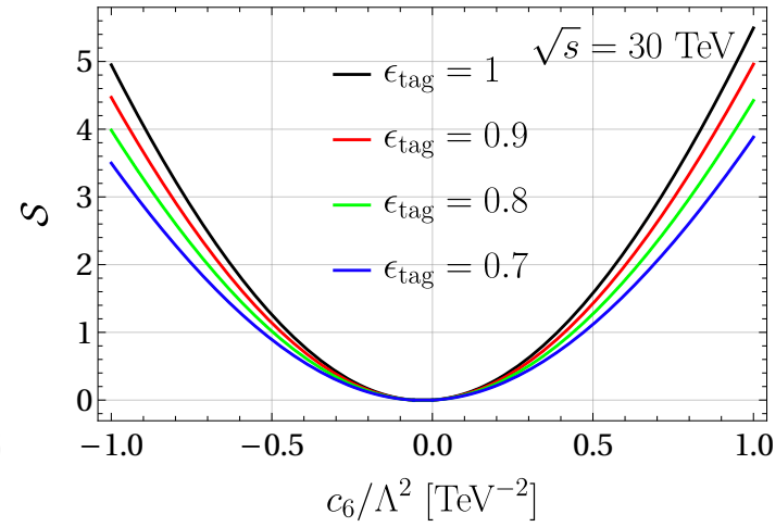
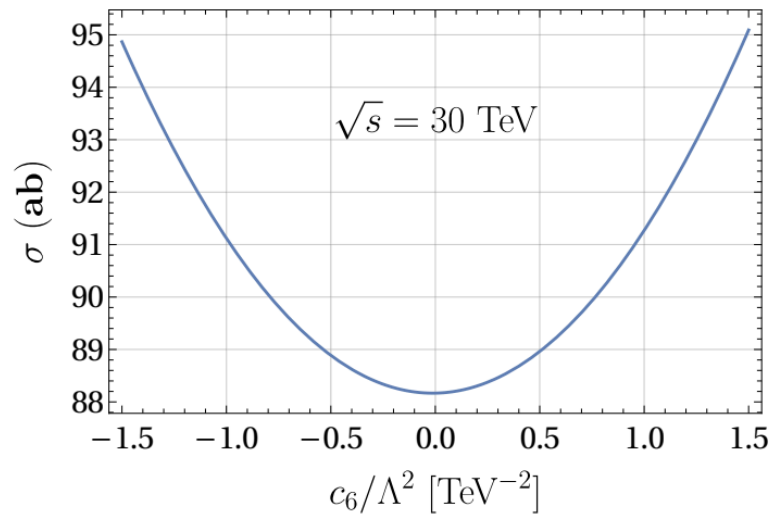
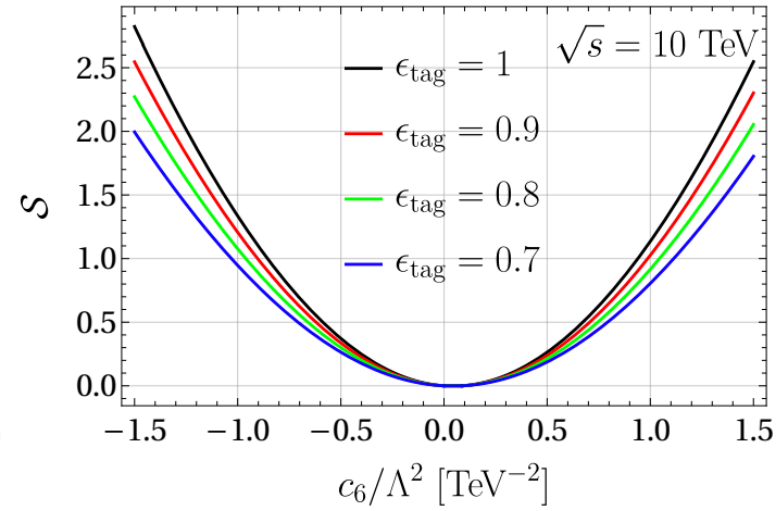
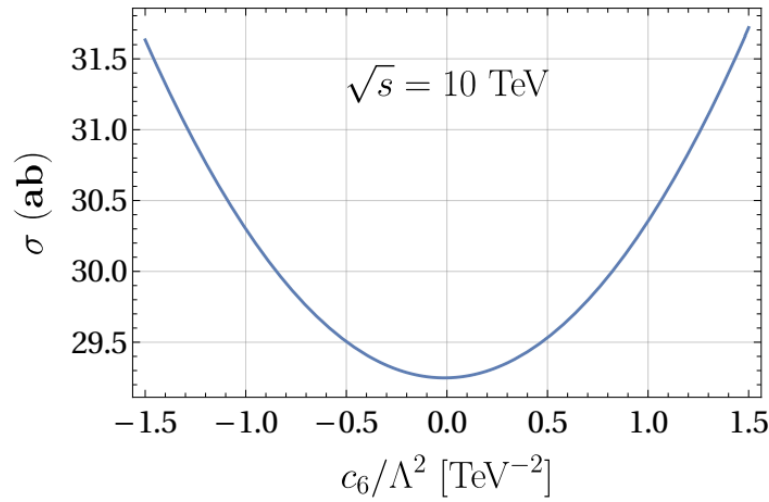
TABLE IV. The summary table of the expected sensitivities to the couplings at  $1\sigma$  and  $2\sigma$  for the three processes  $WWh$ ,  $ZZh$ , and  $hhh$  for  $\sqrt{s} = 10$  TeV and  $\sqrt{s} = 30$  TeV. The tagging efficiency of longitudinal polarizations is assumed to be 100%.

Channels	$\sqrt{s}$ (TeV)	coupling ( $\text{TeV}^{-2}$ )	$1\sigma$	$2\sigma$
$WWh$	10 TeV	$c_6/\Lambda^2$	$[-0.856, 0.940]$	$[-1.245, 1.327]$
		$c_{\Phi_1}/\Lambda^2$	$[-0.318, 0.424]$	$[-0.477, 0.571]$
	30 TeV	$c_6/\Lambda^2$	$[-0.447, 0.389]$	$[-0.627, 0.569]$
		$c_{\Phi_1}/\Lambda^2$	$[-0.0378, 0.0657]$	$[-0.0591, 0.0867]$
$ZZh$	30 TeV	$c_6/\Lambda^2$	$[-1.329, 1.136]$	$[-1.881, 1.691]$
		$c_{\Phi_1}/\Lambda^2$	$[-0.0688, 0.0852]$	$[-0.103, 0.119]$
$hhh$	10 TeV	$c_6/\Lambda^2$	$[-0.926, 0.796]$	$[-1.316, 1.201]$
		$c_{\Phi_1}/\Lambda^2$	$[-0.282, 0.351]$	$[-0.430, 0.505]$
	30 TeV	$c_6/\Lambda^2$	$[-0.354, 0.342]$	$[-0.493, 0.458]$
		$c_{\Phi_1}/\Lambda^2$	$[-0.0324, 0.0576]$	$[-0.0545, 0.0760]$

Results after decaying and background analysis.



# Significance with varying helicity tagging efficiency



# Conclusions

- $2 \rightarrow 3$  VBS includes:  $V_L V_L \rightarrow V_L V_L h$ ,  $V_L V_L \rightarrow h h h$
- Amplitude of  $2 \rightarrow 3$  VBS is very sensitive to new physics on higgs self-couplings.
- Special settings in data and analysis:  
1)select long. pol.; 2)impose PT cuts
- $W^+ W^- \rightarrow W^+ W^- h$  and  $W^+ W^- \rightarrow h h h$ . are good channels to measure Higgs self-couplings, in 100 TeV pp collider, and especially future muon colliders.
- Similar analysis can be applied to top Yukawa(working on progress)

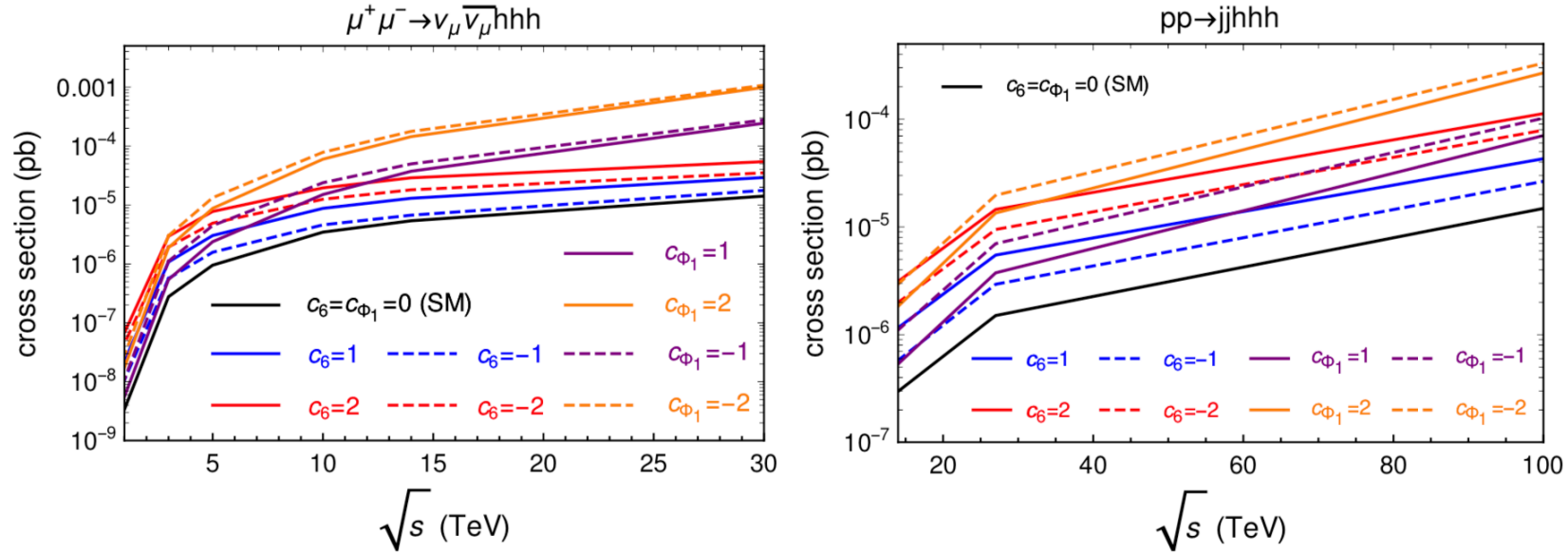


**Figure 9:** The vary of cross sections for  $c_6 = \pm 1, \pm 2$  with  $c_{\Phi_1} = 0$  and  $c_{\Phi_1} = \pm 1, \pm 2$  with  $c_6 = 0$  for  $\mu^+\mu^- \rightarrow \nu_\mu \bar{\nu}_\mu hhh$  from  $\sqrt{s} = 1$  to 30 TeV (left panel) and  $pp \rightarrow jjhhh$  from  $\sqrt{s} = 14$  to 100 TeV (right panel).

Cross section for final hhh sensitive to  $c_6$  and  $c_{\Phi_1}$ .